NOTE

Glimpsing the 2020 spring bloom in the Strait of Georgia (Canada) with autonomous ferry-based sensors

Liam MacNeil[1,3,*], Maycira Costa[2], Julie LaRoche[1]

[1]Biology Department, Dalhousie University, 1355 Oxford St, Halifax, NS B3H 4J1, Canada
[2]Department of Geography, University of Victoria, 3800 Finnerty Rd, PO Box 1700, Victoria, BC V8W 2Y2, Canada

[3]*Present address:* GEOMAR Helmholtz Centre for Ocean Research Kiel, Wischhofstraße 1–3, 24148 Kiel, Germany

ABSTRACT: Spatiotemporal observations are data rich and offer insights into links between ecological patterns and underlying processes. We present fine-scale autonomous observations from repeated ferry transects in the Strait of Georgia (British Columbia, Canada) during the 2020 spring bloom period using a FerryBox system (temperature, salinity, chlorophyll *a* fluorescence) and a digital inline holographic microscope. Despite instrument cleaning interruptions related to COVID-19 restrictions, 3 periods from late winter (February) to springtime (March and April) contained 14 days of high-quality holograms (>70 000) capturing >10 500 identifiable micro- to mesoplankton using automatic object detection. The ferry set-up provided automatic data storage through Ocean Networks Canada, which also automatized data flagging and guaranteed remote access. The highest-quality holograms repeatedly covered the central and eastern Strait and showed aspects of bloom succession. Fast-growing diatoms (*Skeletonema* sp.) emerged first, followed by a diverse assemblage including *Chaetoceros* spp., *Ditylum* spp., and *Eucampia* spp., and by April, larger centric cells prevailed. The combined approach captured local suppression of chlorophyll *a* fluorescence and diatom concentrations in Fraser River plume waters during the freshet, suggesting fine-scale spatial patterns in seasonal planktonic community composition. This work is among the first of its kind to autonomously generate *in situ* imaging and physicochemical data with spatiotemporal resolution.

KEY WORDS: Automated ferry sampling · Holographic imaging · Plankton · FerryBox · Strait of Georgia · Salish Sea

1. INTRODUCTION

Coastal ecosystems comprise the most biologically productive marine zones on Earth (Behrenfeld et al. 2006). On the Pacific continental shelf in the semi-enclosed Salish Sea, the Strait of Georgia (Canada) is a productive and biodiverse estuary that has become one of the most human-dominated marine ecosystems in Canada (Perry & Masson 2013). Estuarine circulation features tidal and wind-driven mixing in the

Strait with terrestrial freshwater run-off dominated by the Fraser River — the largest point source of suspended particulate matter entering the Pacific Ocean from Canada (Thomson 1981). Plankton blooms in this region are complex, where timing and distribution are considered bottom-up controls on zooplankton production and recruitment of multiple fish species (e.g. Perry et al. 2021). Spring blooms range from late winter to early summer, strongly influenced by winter stratification before the Fraser River freshet,

*Corresponding author: lmacneil@geomar.de

and display spatial structure in seasonal bloom evolution (Halverson & Pawlowicz 2013). Generally, spring blooms are dominated by diatoms such as *Skeletonema* sp., *Thalassiosira* spp., and *Chaetoceros* spp., followed by a succession of flagellates in summertime (Harrison et al. 1983, Del Bel Belluz et al. 2021), but high-frequency *in situ* observations with spatiotemporal and taxonomic resolution are lacking.

In highly trafficked coastal environments, networks of non-scientific vessels remain underused for the collection of biological data. The European Global Ocean Observing Network has implemented flow-through FerryBoxes on ferry and cargo vessels to autonomously obtain physical (temperature, salinity, turbidity), chemical (nutrients, pH, CO_2, dissolved organic carbon), and biological (chlorophyll *a* [chl *a*] fluorescence) observations near continuously from surface waters (Petersen 2014). Our work describes fine-scale autonomous biological observations from repeated ferry transects in the Strait of Georgia during the 2020 spring bloom period (February–April) using a FerryBox system and a high-throughput plankton imaging device to capture taxonomic composition and size structure. Among the first of its kind, supported by autonomous data collection and storage, plus automatic quality control of physicochemi-cal data, this work provides an outlook of the challenges and prospects for the deployment of plankton imaging systems aboard ferry platforms.

2. MATERIALS AND METHODS

2.1. Autonomous ferry observations

A British Columbia Ferry Services Inc. vessel, the MV 'Queen of Alberni' double-ended car ferry (139 m), crosses the Strait of Georgia between Duke Point (Vancouver Island) and Tsawwassen (mainland British Columbia) up to 8 times per day (Fig. 1). The Tsawwassen–Duke Point line arcs northwest/southeast roughly 70 km with a maximum transit speed of 21 knots. An autonomous FerryBox system is operated by Ocean Networks Canada (ONC) for high-frequency records of temperature, salinity, chl *a* fluorescence, and oxygen (Halverson & Pawlowicz 2013, Wang et al. 2019). Subsurface water intake is continuous at 2 m (±40 cm) below the water line from a 12.7 mm opening into a pump and valve control system directing water through a 1.5 m pipe 10 m from the bow. Water intake is automatically turned off at speeds <5 knots to prevent contamination in harbor, especially from particu-
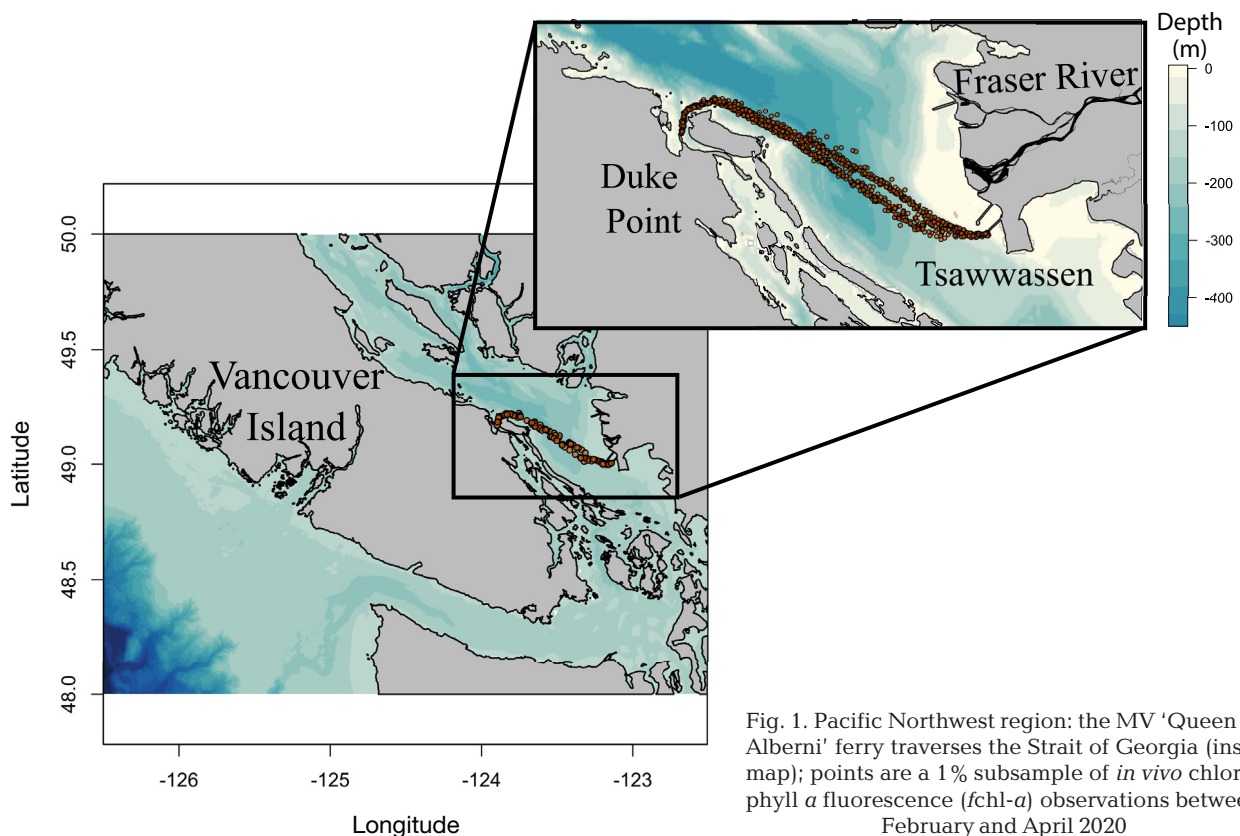

Fig. 1. Pacific Northwest region: the MV 'Queen of Alberni' ferry traverses the Strait of Georgia (inset map); points are a 1% subsample of *in vivo* chlorophyll *a* fluorescence (*f*chl-*a*) observations between February and April 2020

late matter discharged from the Fraser River, ~15 km north of the Tsawwassen dock. For this work, we incorporated FerryBox data, including a thermosalinograph measuring at 5 s intervals (SBE 45), a fluorometer measuring *in vivo* chl *a* fluorescence (*f*chl-*a*) and chromophoric dissolved organic matter (CDOM) fluorescence every 2 s (WET Labs ECO Triplet fluorometer), and a GPS measuring every 10 s (Thrane and Thrane Sailor navigational sensor). The full FerryBox data set summed from 924 transects, spanning February— June, produced >346 000 observations (Text S1 and Fig. S1 in the Supplement at www.int-res.com/articles/suppl/m736p181_supp.pdf).

To directly image micro- to mesoplankton, a digital in-line holographic microscope (4-Deep HoloSea S7; 92 × 351 mm, 2.6 kg) was mounted horizontally within a flow-through chamber (4.59 l) and integrated into the pump and valve control system (Fig. S2). Immersing the HoloSea in seawater ensured cooling and prevented condensation on the lens. The HoloSea S7 uses a complementary metal oxide semiconductor (CMOS) camera (MV1-D2048-96-G2-10 Photonfocus) with 7.4 µm pixel resolution to record interference patterns (2048 × 2048 pixels) from a single coherent light source (386 nm; 0.5 µs pulses; 10 frames per second in 100 s bursts). Numerical reconstruction of wavefront point intensities throughout the depth-of-field was computed based on a Helmholtz-Kirchhoff transformation, in-focus object detection from holograms used a moving background subtraction, global threshold-clustering, and neighboring correlative algorithm (size range ~10— 2000 µm diameter; MacNeil et al. 2021). Detected objects were curated manually for plankton and particulates (aggregates, marine snow, etc.) and identified to the lowest possible taxonomic rank (Table S1). Concentrations were calculated based on the fraction of volume imaged, calculated by multiplying the number holograms by the effective volume per hologram (0.063 ml; Table S2). Plankton size estimates (equivalent spherical diameter) were derived from feature extraction in the 'OpenCV' toolbox (Bradski 2000) and corrected for object location in sample space based on light diffraction (Walcutt et al. 2020).

Automated holographic imaging typically occurred during 1 transect per day, with ~1.9 km spatial resolution and averaging 5000 holograms (>20 GB) per transect from 25 February through 30 August 2020. To analyze higher-quality holograms, we selected transects collected soonest after cleaning events where hologram illumination was unobstructed by biofouling; this included 15 transects (25 February to 16 April) and >70 000 holograms (>310 GB).

2.2. Data storage and quality control

Biofouling occurred rapidly in this highly productive and turbid region (Fig. S3). Planned bi-weekly maintenance and cleaning trips were disrupted by COVID-19 public restrictions and limited cleaning episodes to 3 during imaging campaigns (25 February, 20 March, 9 April). Limited cleaning impaired data quality across all sensors due to biofouling throughout summer and autumn and resulted in relatively patchy, but nonetheless data-rich, samples.

The FerryBox sensors are privileged to automatic data quality controls by ONC, including spike detection and gradient steepness tests (Owens et al. 2022). All FerryBox data were selected against the ONC data quality flag scheme for identifiers 1 (passed all quality control tests) and 2 (probably good) and calculated as 1 min averages. A linear biofouling correction factor was applied to *f*chl-*a* based on instrument benchmarking against a standard solution (Table S3). Data products were stored automatically in real time via a static IP connection onto the network-attached storage (Synology 37 TB) installed on the ferry, ensuring quality control checks and that units were parsed before being sent onto database storage (Owens et al. 2022). Holograms were automatically stored onboard and uploaded manually to onshore storage. All data products were downloaded freely from the Oceans 3.0 data portal (https://data.oceannetworks.ca/home).

3. RESULTS

The combination of FerryBox variables depicts seasonal evolution from late wintertime through early summer at high spatiotemporal resolution (Fig. 2A). Seasonality showed substantial average changes including surface seawater warming (6 to 16°C), a springtime freshet that dramatically reduced salinity (30 to 5 PSU) accompanied by elevated CDOM concentrations (4 to 10 ppb) and reduced *f*chl-*a* (5 to 1 µg l^{-1}). The spring bloom (*f*chl-*a*) was apparent after the second week of March, with a secondary peak in late March (Fig. S1). Ferry tracks revealed a spatial pattern where the eastward section of the Strait became dominated by the Fraser River freshet conditions, displaying fresher and less productive waters with high concentrations of CDOM (Fig. 2A). In turn, the spring bloom was highest on average in the westward sections of the Strait (Fig. 2A).

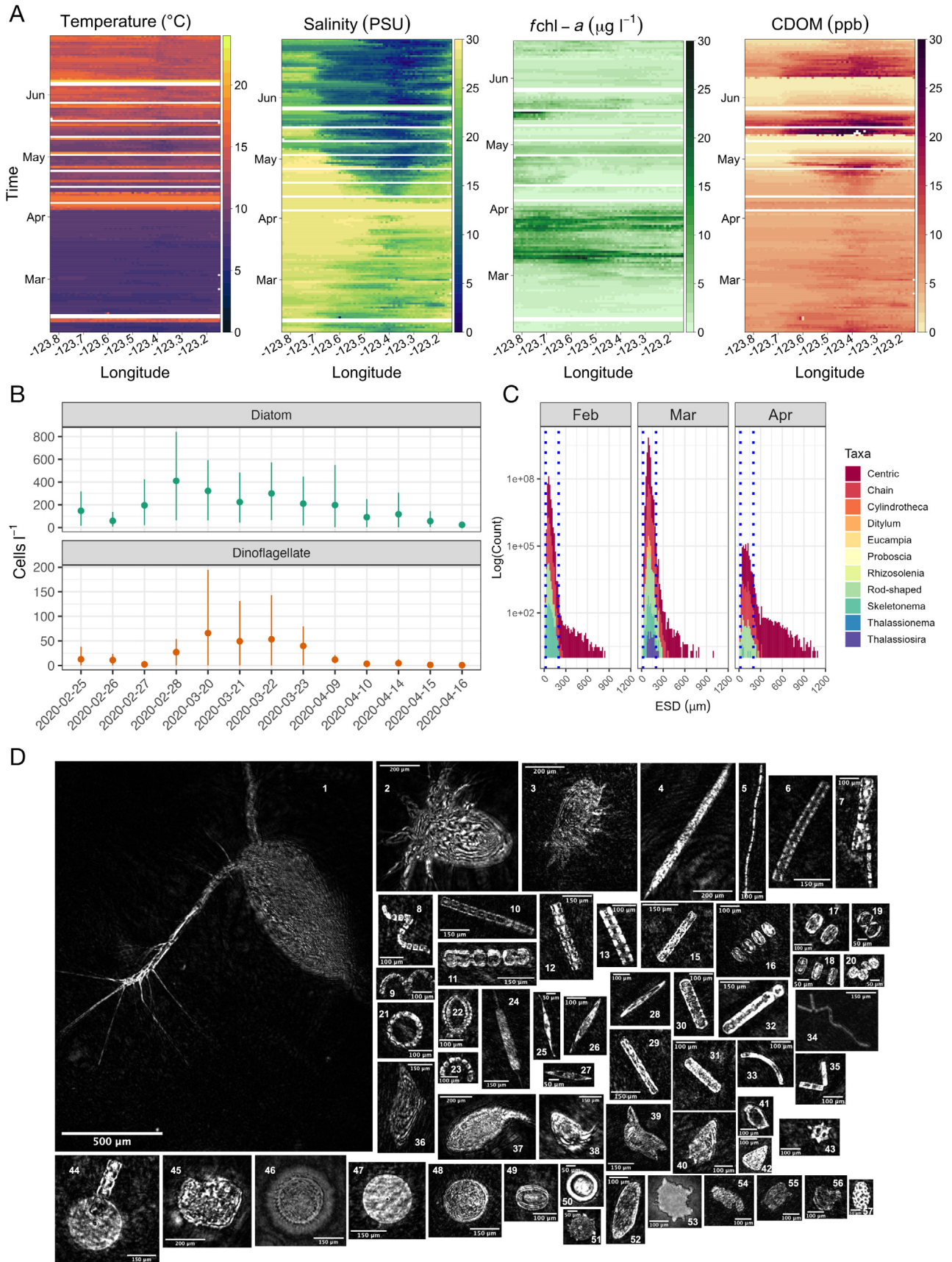The object-detection algorithm totaled ~250 h of computation time, detecting >12 000 in-focus ob-

Fig. 2. Ferry-based observations from (A) the FerryBox shown in Hovmöller diagrams covering 1 February to 30 June 2020. Arranged spatiotemporally, the *x*-axes display the cross-strait space (left to right: Duke Point to Tsawwassen) against time for each variable (*in vivo* chlorophyll *a* fluorescence, *f*chl-*a*; chromophoric dissolved organic matter, CDOM) at 1 min averages, where horizontal gaps represent sampling interruptions. (B) Summary of holographic plankton compositions at each date for the dominant phytoplankton calculated as bootstrap means with 95% confidence intervals. (C) Diatom size distributions (equivalent spherical diameter, ESD) by month including vertical blue lines bounding microplankton (20—200 µm) size class. (D) Collage of high-quality plankton objects detected throughout the 2020 springtime. Plankton are arranged broadly by size, shape, and taxonomic grouping: Adult (1) and larval copepods (2—3), rod-shaped and chained diatoms (4—34) including *Proboscia* sp. (4), *Skeletonema* sp. (5) large chains (>300 µm; 6—7, 10—11), *Chaetoceros* sp. (8—9), *Odontella* sp. (12—13), smaller chains (<300 µm; 15, 19—20, 23), *Thalassiosira* sp. (16—18), *Eucampia* sp. (21—22), *Ditylum* sp. (24), *Nitzschia* sp. (25—27), other pennate diatoms (28—33), *Thalassionema* sp. (34—35), and *Licmophora* sp. (36). Dinoflagellates (37—41) included *Tripos* sp. (39) and *Prorocentrum* sp. (41). Silicoflagellate *Dictyocha* sp. (42) and ciliates (43) were also present. Centric diatoms (44—50) lacked taxonomically diagnostic features. A diverse collection of particulates and marine snow were also detected (51—57), potentially containing microplastics (53)

jects of which 10 500 were taxonomically identifiable plankton (Fig. S4). Diatoms dominated compositions (>90%) with 10 genera, followed by dinoflagellates (4%) with 2 resolvable genera (Fig. 2D). Other groups, including copepods, tintinnids, rotifers, and silicoflagellates, were rare. Highest-quality holograms were recorded before (28 February) and during the secondary spring bloom peak (20—23 March), capturing high diatom concentrations (mean ± SD = 1143 ± 501 cells l^{-1}, Fig. 2B), but were limited in spatiotemporal resolution (Figs. S5 & S6).

The westward section of the Strait where *f*chl-*a* peaked during the spring bloom was not sufficiently covered by imaging due to limited cleaning access, which hampered image quality. However, the western section was covered in April, where diatom concentrations appeared negatively associated with plume water features (low salinity, high CDOM; Fig. S7). In the central and eastern sections of the ferry route, phytoplankton composition shifts were apparent across imaging events, with February compositions dominated by smaller chains (*Skeletonema* sp.). March was characterized by unresolvable rod-shaped taxa, *Proboscia* spp., with few microplankton chains (*Thalassiosira* spp., *Chaetoceros* spp.), and by April, a transition occurred to large (>200 µm) centric species (Fig. 2B,C). Phytoplankton sizes also increased throughout spring, averaging 111.6 ± 105.2 µm to 232.7 ± 162.4 µm in February and April, respectively.

4. DISCUSSION

Spatiotemporal observations provide a basis for recording ecological and environmental processes in the dynamic marine realm. We provide among the first examples of autonomous spatiotemporal plankton imaging, enhanced by 3D holographic reconstruction, automatic object detection, and paired to high-throughput physicochemical measurements. Automatic data storage unique to the FerryBox and imaging systems accelerated data acquisition, automatized data flagging, and guaranteed remote access through the Oceans 3.0 data portal. Although this was an exploratory project, the central and eastern section of the Strait were repeatedly sampled (Figs. S5 & S6) during springtime, with high quality data from late February to mid-April.

Within this time series, indications of bloom succession were apparent. Fast-growing diatoms (*Skeletonema* sp.) emerged first while average *f*chl-*a* remained low (<1 µg l^{-1}), followed in mid-March by a more diverse assemblage including *Chaetoceros* spp., *Ditylum* spp., and *Eucampia* spp. during the spring bloom (average *f*chl-*a* >5 µg l^{-1}). By April, generally larger centric cells prevailed in imaging compositions, while *f*chl-*a* shows the spring bloom subsiding (average *f*chl-*a* <3 µg l^{-1}), especially in the eastward section of the Strait. Diatoms are known to dominate spring blooms in this region (Harrison et al. 1983, Del Bel Belluz et al. 2021), supporting our general seasonal pattern in surface waters derived from automatic holographic imaging. This work extends this knowledge to include patterns in size structure, which remain less well documented in space and time.

The Fraser River plume suppresses planktonic productivity by limiting light penetration into the water column; however, its frontal boundaries can create zones of high productivity, likely due to vertical mixing and relatively greater light availability (Yin et al. 1997), which our results support but with limited evidence (Fig. S6). Although *f*chl-*a* broadly captured the spatial dynamics of the Fraser River freshet and

the imaging concentrations reflected plume water properties, their weak correlation (Pearson r < 0.2) was due to intense instrument fouling, evidenced by one-fifth of $f$chl-a readings being flagged unreliable and removed. More broadly, the daily spatial structuring of planktonic productivity by plume waters suggests similar effects for community composition which we are yet unable to resolve, but our approach could capture its spatial variability if increased in frequency.

Numerous factors need improvement for future ferry-based deployments. Firstly, *in situ* chl *a* samples are needed to calibrate *in vivo* fluorescence readings and correct for diurnal non-photochemical quenching (unrealized in 2020 due to public restrictions; Halverson & Pawlowicz 2013). Secondly, sustained bi-weekly cleaning procedures are necessary, especially during the freshet (April–June), to reliably relate imaging concentrations to $f$chl-a, which was achieved with this holographic instrument on the Newfoundland Shelf (MacNeil et al. 2022). Thirdly, a combination of multiple object-detection algorithms could overcome their individually biased estimates of prevalence, size, and shape (Giering et al. 2020). Finally, to scale imaging efforts, improvements towards automatic plankton classification will require annotated data sets from the region. Inline holography is desirable because of its simple flow-through design without microfluidics and efficient numerical wavefront reconstruction; however, other imaging modes can now produce high-quality images with or without lenses, and from coherent or collimated light sources with or without illumination gates (Jaffe 2015).

The outlook for autonomous spatiotemporal observation networks in marine ecology is promising. Numerous oceanographic, meteorological, and biological sensors exist in varying stages of maturity, including towed or autonomous underwater vehicles, Lagrangian drifters, depth profilers, gliders, and sail drones (Whitt et al. 2020). Public ferries are easier to access than all of the above and have proven benefits for tracking spatiotemporal patterns in primary productivity (Halverson & Pawlowicz 2013), ground-truthing remote sensing observations (Travers-Smith et al. 2021), and disentangling oceanic carbon source–sink trends (Macovei et al. 2021). At its core, expanding biological and ecological observations through ferry-based networks costs less than remotely operated alternatives and promises rewarding insights into species distributions, seasonality, and their cues in dynamic environments.

LITERATURE CITED

Behrenfeld MJ, O'Malley RT, Siegel DA, McClain CR and others (2006) Climate-driven trends in contemporary ocean productivity. Nature 444:752–755

Bradski G (2000) The OpenCV library. Dr Dobbs J Softw Tools 25:120–126

Del Bel Belluz J, Peña MA, Jackson JM, Nemcek N (2021) Phytoplankton composition and environmental drivers in the Northern Strait of Georgia (Salish Sea), British Columbia, Canada. Estuaries Coasts 44: 1419–1439

Giering SLC, Hosking B, Briggs N, Iversen MH (2020) The interpretation of particle size, shape, and carbon flux of marine particle images is strongly affected by the choice of particle detection algorithm. Front Mar Sci 7:564

Halverson MJ, Pawlowicz R (2013) High-resolution observations of chlorophyll-*a* biomass from an instrumented ferry: influence of the Fraser River plume from 2003 to 2006. Cont Shelf Res 59:52–64

Harrison PJ, Fulton JD, Taylor FJR, Parsons TR (1983) Review of the biological oceanography of the Strait of Georgia: pelagic environment. Can J Fish Aquat Sci 40: 1064–1094

Jaffe JS (2015) Underwater optical imaging: the past, the present, and the prospects. IEEE J Oceanic Eng 40: 683–700

MacNeil L, Missan S, Luo J, Trappenberg T, LaRoche J (2021) Plankton classification with high-throughput submersible holographic microscopy and transfer learning. BMC Ecol Evol 21:123

MacNeil L, Desai DK, Costa M, LaRoche J (2022) Combining multi-marker metabarcoding and digital holography to describe eukaryotic plankton across the Newfoundland Shelf. Sci Rep 12:13078

Macovei VA, Petersen W, Brix H, Voynova YG (2021) Reduced ocean carbon sink in the south and central North Sea (2014–2018) revealed from FerryBox observations. Geophys Res Lett 48:e2021GL092645

Owens D, Abeysirigunawardena D, Biffard B, Chen Y and others (2022) The Oceans 2.0/3.0 Data Management and Archival System. Front Mar Sci 9:806452

Perry RI, Masson D (2013) An integrated analysis of the marine social–ecological system of the Strait of Georgia, Canada, over the past four decades, and development of a regime shift index. Prog Oceanogr 115:14–27

Perry RI, Young K, Galbraith M, Chandler P, Velez-Espino A, Baillie S (2021) Zooplankton variability in the Strait of

Georgia, Canada, and relationships with the marine survivals of Chinook and Coho salmon. PLOS ONE 16: e0245941

Petersen W (2014) FerryBox systems: state-of-the-art in Europe and future development. J Mar Syst 140:4—12

Thomson RE (1981) Oceanography of the British Columbia Coast. Can Spec Publ Fish Aquat Sci 56. https://waves-vagues.dfo-mpo.gc.ca/library-bibliotheque/487.pdf

Travers-Smith H, Giannini F, Sastri AR, Costa M (2021) Validation of non-photochemical quenching corrections for chlorophyll-*a* measurements aboard ships of opportunity. Front Mar Sci 8:686750

Walcutt NL, Knörlein B, Cetinić I, Ljubesic Z and others (2020) Assessment of holographic microscopy for quantifying marine particle size and concentration. Limnol Oceanogr Methods 18:516—530

Wang C, Pawlowicz R, Sastri AR (2019) Diurnal and seasonal variability of near-surface oxygen in the Strait of Georgia. J Geophys Res Oceans 124:2418—2439

Whitt C, Pearlman J, Polagye B, Caimi F and others (2020) Future vision for autonomous ocean observations. Front Mar Sci 7:697

Yin K, Harrison PJ, Beamish RJ (1997) Effects of a fluctuation in Fraser River discharge on primary production in the central Strait of Georgia, British Columbia, Canada. Can J Fish Aquat Sci 54:1015—1024